

# Exceptional Topology on Nonorientable Manifolds

J. Lukas K. König,<sup>1,\*</sup> Kang Yang,<sup>2,\*</sup> André Grossi Fonseca,<sup>3</sup> Sachin Vaidya,<sup>3</sup> Marin Soljačić,<sup>3</sup> and Emil J. Bergholtz<sup>1</sup>

<sup>1</sup>Department of Physics, Stockholm University, AlbaNova University Center, 106 91 Stockholm, Sweden

<sup>2</sup>Dahlem Center for Complex Quantum Systems and Fachbereich Physik, Freie Universität Berlin, 14195 Berlin, Germany

<sup>3</sup>Department of Physics, Massachusetts Institute of Technology, Cambridge, Massachusetts 02139, USA

(Dated: March 1, 2025)

We classify gapped and gapless phases of non-Hermitian band structures on two-dimensional nonorientable parameter spaces. Such spaces arise in a wide range of physical systems in the presence of non-symmorphic parameter space symmetries. For gapped phases, we find that nonorientable spaces provide a natural setting for exploring fundamental structural problems in braid group theory, such as torsion and conjugacy. Gapless phases, which host exceptional points (EPs), explicitly violate the fermion doubling theorem, even in two-band models. We demonstrate that EPs traversing the nonorientable parameter space exhibit non-Abelian charge inversion. These braided phases and their transitions leave distinct signatures in the form of bulk Fermi arc degeneracies, offering a concrete route toward experimental realization and verification.

*Introduction.* — Non-Hermitian phases have been broadly studied in systems where gain and loss are non-negligible, which range from condensed matter to optics, acoustics, and electrical circuits [1–7]. Non-Hermitian bands and their degeneracies, namely exceptional points (EPs) [8–15], often challenge cornerstones of topological physics, such as the fermion doubling theorem [16–19] and the bulk-boundary correspondence [20–24]. This exceptional topology is closely tied to the study of braids and knots [25–32], formed by complex spectra in non-Hermitian phases winding around each other. On orientable parameter spaces, the non-Abelian character of the

braid group has revealed many interesting physically observable consequences, including path-dependent fusions of EPs and spectral flows [33–40]. These observations result from the interplay between the braid group and the underlying topology of the orientable parameter space, typically a torus or a disc.

Recent work on Hermitian systems has shown that more exotic parameter spaces are physically accessible, and that they fundamentally change the topological classification. For example, certain configurations of gauge fluxes or moiré structures in real-space translate into nonsymmorphic symmetries in momentum space and render the Brillouin zone a nonorientable manifold. This enriches topological physics, reducing Chern numbers to  $\mathbb{Z}_2$  symmetry-protected invariants, and modifies fermion doubling, requiring even, but possibly non-vanishing total chirality [41–54].

Such parity requirements are characteristic of Abelian topology on nonorientable spaces. As braids and knots on nonorientable surfaces differ decidedly from those on tori or discs, one may naturally expect richer symmetry-protected non-Hermitian phases and unique, distinctly non-Abelian features to arise in the intersection of non-Hermiticity and nonorientability. In this work, we explore this intersection by investigating how the exceptional topology of gapped and gapless phases fares in nonorientable spaces. We first apply the theory of braided band structures to nonorientable parameter spaces, using as examples the Klein bottle  $\mathbf{K}^2$  and the real projective plane  $\mathbf{RP}^2$ . We find a system of phases classified by two (one) braid, respectively, and derive the modifications to the fermion doubling theorem on these spaces. Second, we discuss gapped phases, of which we find an infinite family on  $\mathbf{K}^2$ , and show how these can be distinguished by a non-Hermitian Fermi arc structure. Third, we show that gapless systems can be identified by a new kind of unpaired monopole that is forbidden both in Hermitian systems and in non-Hermitian systems on orientable spaces. Finally, we discuss phase transitions, which occur when EPs encircle the parameter space. We provide concrete rules how the encircling EP and the topological phase affect each other. Our work provides insights into how non-Hermiticity and nonorientability interact to produce unique topological phases, expanding the

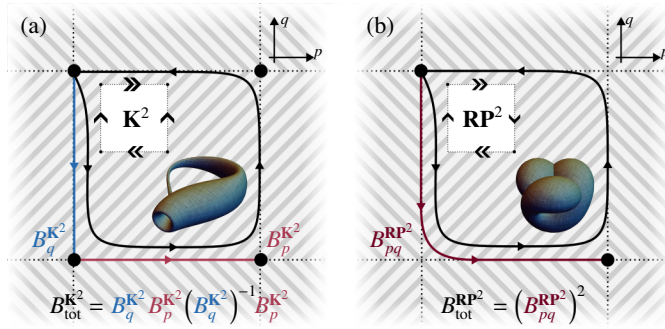


**Figure 1.** Exceptional phases on nonorientable manifolds: Under the boundary identification shown in the top-left insets, a free parameter space becomes (a) the Klein bottle, (b) the real projective plane, illustrated as an immersion into  $\mathbb{R}^3$  in the bottom-right insets. The red and blue paths become non-contractible loops in the space, and generate its fundamental group. The *total* black loop enclosing the fundamental domain is a combination of these fundamental loops. Non-Hermitian exceptional phases are identified by the braiding of spectra along the fundamental loops. Statements about their separation gap can be made from the total braid along the black loop, following Eq. (2). Background shading denotes the orientation of the neighboring unit cells.

\* These authors contributed equally to this work

boundaries of non-Hermitian topological band theory.

**Braid Topology Recap.** — In an  $m$ -band system, the eigenvalue winding along a parametric loop determines a braid, an element of the Artin braid group  $\mathbb{B}_m$ . Arbitrary braids can be composed out of pairwise counterclockwise exchanges of bands  $E_i, E_{i+1}$  in the complex plane, called  $\sigma_i \in \mathbb{B}_m$ , as well as their inverses [55]. The eigenvalue topology in a two-dimensional parameter space is entirely determined by such braids along the space's non-contractible loops [26–28, 32]. Here we consider two particular spaces which exemplify the generic features of nonorientable fundamental domains; the Klein bottle  $\mathbf{K}^2$ , and the real projective plane  $\mathbf{RP}^2$ . A  $\mathbf{K}^2$  fundamental domain arises for example from an originally  $2\pi$ -periodic operator  $H(p, q) = H(p + 2\pi, q) = H(p, q + 2\pi)$  by imposing a non-symmorphic parameter space symmetry of the form

$$H(p, q) = H(-p, q + \pi), \quad (1)$$

which reduces the fundamental domain to  $[-\pi, \pi] \times [0, \pi]$ .  $\mathbf{RP}^2$  arises under an additional non-symmorphic symmetry of the same form, with the roles of  $p$  and  $q$  reversed, which reduces the fundamental domain to  $[-\pi/2, \pi/2] \times [-\pi/2, \pi/2]$ . Note that the non-Hermitian parameter spaces can be momentum space, quasimomentum space, or more generic parameter spaces depending on the physical platform, and are therefore parametrized by generic  $p, q$  in this work [11, 56–59].

On these spaces there are, respectively, two and one distinct non-contractible loops (see Figure 1). We index their topological phases by the corresponding braids, i.e.,  $(B_p^{\mathbf{K}^2}, B_q^{\mathbf{K}^2})$  and  $B_{pq}^{\mathbf{RP}^2}$ , along these non-contractible loops. Transitions between different phases indexed by different braids require band gap closings and happen via EPs that travel along a path encircling the fundamental domain.

Here we classify two types of phases, band gapped and gapless, depending on whether potentially occurring EPs can pair-annihilate and gap out locally. This is determined following the braid of eigenvalues along loops enclosing the whole fundamental domain  $B_{\text{tot}} = \prod_i B_{\text{EP},i}$  (see Figure 1), which equals the combined charge of all EPs in the system. For a band gapped system,  $B_{\text{tot}}$  must be trivial, while a non-trivial  $B_{\text{tot}}$  necessitates gap-closings, i.e., EPs in the band structure [19]. Since  $B_{\text{tot}}$  encloses the fundamental domain, its structure is determined by the underlying space. On a torus this means that the total braid has the shape of a braid group commutator  $B_{\text{tot}}^{\mathbf{T}^2} = B_q^{\mathbf{T}^2} B_p^{\mathbf{T}^2} (B_q^{\mathbf{T}^2})^{-1} (B_p^{\mathbf{T}^2})^{-1}$  in the phase  $(B_p^{\mathbf{T}^2}, B_q^{\mathbf{T}^2})$  [27, 28], while on the nonorientable manifolds we study here, it is made up of constituent braids as (see in Figure 1)

$$B_{\text{tot}}^{\mathbf{K}^2} = B_q^{\mathbf{K}^2} B_p^{\mathbf{K}^2} (B_q^{\mathbf{K}^2})^{-1} B_p^{\mathbf{K}^2}, \quad B_{\text{tot}}^{\mathbf{RP}^2} = (B_{pq}^{\mathbf{RP}^2})^2. \quad (2)$$

These equations (and the commutator on the torus) imply that the sum of all EP invariants must take a specific form. Crucially, unlike on the orientable torus,  $B$  and its inverse  $B^{-1}$  do not appear in pairs in these expressions.

We first investigate the consequence of such total braids on two-band models, where the two-strand braid group is equivalent to its Abelianization, the vorticity of eigenvalue braidings

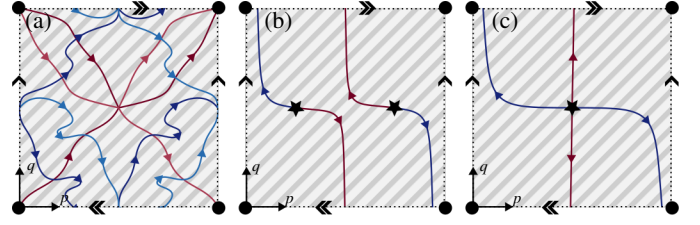


**Figure 2.** Fermi arcs as experimentally accessible signatures. Real (imaginary) Fermi arcs as defined in Eq. (7) are drawn in red (blue), with the orientation defined in the main text. (a) the gapped three-band model on  $\mathbf{K}^2$  given in Eq. (6), with lighter and darker tones denoting Fermi arcs of different band pairs. The exceptional phase, identified by the braids  $(\sigma_2 \sigma_1^{-1}, \Delta^{-1})$  along the  $p$ - and  $q$ -directions, has three Fermi arcs encircling the fundamental domain in the positive  $p$ -direction, originating from the Abelianization of  $\Delta$ . This clearly distinguishes this phase from the trivial flat-band phase  $(1, 1)$ . (b) the two-band model in Eq. (8) at  $\ell = 0$ , perturbed to  $e^{0.02i} H_{\text{EP}}^{\mathbf{K}^2}$  to better showcase the Fermi arcs. A real and an imaginary Fermi arc emerge from each EP (star marker), with a direction given by the eigenvalue crossing behavior. This direction is inverted on the nonorientable boundary, allowing for a total flux out of the fundamental domain that matches the total braid degree, 2. (c) the two-band model in Eq. (8), perturbed as in (b) and tuned to  $\ell = 1$  exhibits a characteristic monopole. Two real and two imaginary Fermi arcs emerge from the monopole, accounting for its total braid degree  $A_{\text{tot}}^{\mathbf{K}^2} = 2$ . Such an EP cannot exist alone on an orientable space, where outgoing Fermi arcs cannot be compensated.

[26]. Given some braid  $B$ , its Abelianization  $A \in \mathbb{Z}$ , also known as the degree of  $B$ , is the difference between its number of overcrossings and undercrossings [19, 32, 60]. In particular, the consistency conditions for the total braid simplify to sums over these numbers. While the Abelianized relation on the torus reads simply  $A_{\text{tot}}^{\mathbf{T}^2} = 0$ , the total Abelianized invariants on non-orientable spaces may be non-zero, satisfying

$$A_{\text{tot}}^{\mathbf{K}^2} = A_q^{\mathbf{K}^2} + A_p^{\mathbf{K}^2} - A_q^{\mathbf{K}^2} + A_p^{\mathbf{K}^2} = 2A_p^{\mathbf{K}^2}, \quad A_{\text{tot}}^{\mathbf{RP}^2} = 2A_{pq}^{\mathbf{RP}^2}. \quad (3)$$

This is reminiscent of the Hermitian case, where only the parity of the Chern number is physically meaningful on nonorientable spaces [42], which leads to a  $\mathbb{Z}_2$  fermion doubling theorem in three dimensions [41]. This Abelian description is the full picture for two-band models. For three or more bands, the full description of nonorientable topological phases needs more non-Abelian information.

**Gapped Phases and Fermi Arcs.** — We begin by describing those phases that can be gapped, for which we have  $B_{\text{tot}} = 1$ . On the torus, this necessitates that the braids  $B_p^{\mathbf{T}^2}$  and  $B_q^{\mathbf{T}^2}$  commute [27, 28], which in particular implies zero total Abelianization, reminiscent of the original formulation of fermion doubling [16, 17]. A gapped phase on  $\mathbf{RP}^2$  must instead satisfy  $1 = (B_{pq}^{\mathbf{RP}^2})^2$  following Eq. (2). This condition amounts to finding braid elements that square to unity ( $\mathbb{Z}_2$  torsion). Since the braid group is torsion-free [60], we have

$$B_{pq}^{\mathbf{RP}^2} = 1, \quad (4)$$

Hence, all gapped phases on the real projective plane share a trivial braid.

Gapped phases on the Klein bottle are classified by setting  $B_{\text{tot}} = 1$  in Eq. (2)

$$B_p^{\mathbf{K}^2} = B_q^{\mathbf{K}^2} (B_p^{\mathbf{K}^2})^{-1} (B_q^{\mathbf{K}^2})^{-1}, \quad (5)$$

i.e., the braid  $B_p^{\mathbf{K}^2}$  must be conjugate to its own inverse, with the braid  $B_q^{\mathbf{K}^2}$  as the conjugating element. For a two-band system, we can solve this equation using its Abelianization. This requirement reads  $A_p^{\mathbf{K}^2} = 0$ , i.e., zero braid degree along the  $p$ -boundary. So two-band gapped phases must thus have trivial  $B_p^{\mathbf{K}^2} = 1$ , and are solely indexed by a free choice of  $B_q^{\mathbf{K}^2}$ .

For systems of three or more bands, we need to solve the non-Abelian conjugacy question, which is a key braid group structure and usually very complicated. An example of a non-trivial solution is  $B_p^{\mathbf{K}^2} = \sigma_2 \sigma_1^{-1}$ . This braid is indeed conjugate to its own inverse, i.e., it satisfies Eq. (5) for the choice  $B_q^{\mathbf{K}^2} = \Delta = \sigma_1 \sigma_2 \sigma_1$ .  $\Delta$  is the fundamental braid on three strands, which plays an important role in the study of braid groups [60]. Conjugation with  $\Delta$  is equivalent to flipping a braid upside down, i.e., replacing  $\sigma_1 \leftrightarrow \sigma_2$ ,  $\sigma_1^{-1} \leftrightarrow \sigma_2^{-1}$ , which transforms the choice of  $B_p^{\mathbf{K}^2}$  given here into its inverse.

In stark contrast to classifying gapped phases on the torus, which is solved by mutually commuting braids, gapped phases on nonorientable surfaces bring us to two fundamental structural questions in braid group study, torsion and conjugacy class. Moreover, setting the constituent braids on the torus to those derived above for the Klein bottle,  $(B_p^{\mathbf{T}^2}, B_q^{\mathbf{T}^2}) = (\sigma_2 \sigma_1^{-1}, \Delta^{-1})$  leads instead to a gapless phase containing EPs. A different way to compare the two is to construct a torus out of two copies of  $\mathbf{K}^2$ , by gluing them along the nonorientable boundary. In that scenario, all gapped phases on  $\mathbf{K}^2$  are also gapped on the torus, but conversely there exist gapless phases on  $\mathbf{K}^2$  that can be gapped on the torus, such as all phases with nonzero degree in  $B_p$  and trivial/commuting  $B_q$ .

A model that realises this Klein bottle gapped phase  $(\sigma_2 \sigma_1^{-1}, \Delta^{-1})$  in an experimentally accessible [61] parameter regime is given by

$$H_{\text{gap}}^{\mathbf{K}^2} = \begin{pmatrix} -a & 1 & 0 \\ 1 & b & 1 \\ 0 & 1 & a \end{pmatrix}, \quad \text{where} \quad \begin{cases} a & = i - ie^{2iq} \cos p, \\ b & = (1 + i) e^{3iq} \sin p. \end{cases} \quad (6)$$

Such braided phases can be detected experimentally by their Fermi arcs. In the non-Hermitian regime, Fermi arcs refer to lines of bulk degeneracies in the real or imaginary parts of the spectrum [62], i.e., the lines in parameter space where

$$\text{Re}(E_i - E_j) = 0 \quad \text{or} \quad \text{Im}(E_i - E_j) = 0 \quad (7)$$

for some pair of eigenvalues  $E_i, E_j$  (see Figure 2). Fermi arcs in phases with non-trivial braids are irremovable: As a braid  $\sigma_i$  swaps two eigenvalues along the direction  $p$  or  $q$ , both a real and imaginary Fermi arc must be present. As there are no

EPs in a gapped phase, the Fermi arcs form closed loops in parameter space.

Fermi arcs can be oriented consistently, such that eigenvalues swap places clockwise when crossing the Fermi arc left-to-right. This corresponds to distinguishing crossings  $\sigma_i$  from their inverses. Signed counting of oriented Fermi arcs along a loop thus allows access to a braid's degree. The orientation reversal across a nonorientable boundary implies that a Fermi arc's orientation is reversed on crossing. In order to form closed loops with a consistent orientation, Fermi arcs in gapped phases must therefore cross nonorientable boundaries an even number of times. This is also reflected in the fact that the corresponding braid degrees in Eq. (3) must be trivial.

We note that experimentally determining which eigenvalues cross at a Fermi arc, together with its orientation, allows one to single out a braid group element  $\sigma_i^{\pm 1}$ , and thus completely reconstruct the full braid group description.

*Gapless Systems and Monopole.* — We now describe gapless phases, where the total braid charge over all EPs  $B_{\text{tot}} \neq 1$ . Such a non-trivial  $B_{\text{tot}}$  implies the existence of EPs that cannot annihilate locally in parameter space, violating the fermion doubling theorem. From Eq. (3), we see that on nonorientable spaces  $B_{\text{tot}}$  is allowed to have non-zero even degree, which goes beyond what is possible in non-Hermitian systems on the torus. This is clearly illustrated by fusing all EPs in the system into a single multi-level degeneracy in the parameter space, resulting in a characteristic monopole with charge  $B_{\text{tot}}$ .

We illustrate a two-band gapless  $(\sigma_1, 1)$ -phase on the Klein bottle with the model

$$H_{\text{EP}}^{\mathbf{K}^2} = \begin{pmatrix} -a & 1 \\ 1 & a \end{pmatrix}, \quad (8)$$

for  $a = \sin p \cos q + i(1 - \cos(p))(1 + \ell \cos(2q)/2)$ , and  $\ell \in [0, 1]$  an adiabatic parameter. At  $\ell = 0$ , there are two EPs in this band structure, at  $(p, q) = (\pm\pi/2, \pi/2)$ . Both have the same braid invariant  $\sigma_1$ , summing to  $B_{\text{tot}}^{\mathbf{K}^2} = \sigma_1^2$ . We can achieve the aforementioned fusion to a single monopole by tuning to  $\ell = 1$ , merging the two EPs to a  $\sigma_1^2$ -monopole at  $(p, q) = (\pi, \pi/2)$  (see Figure 2). This is an unpaired monopole and has total braid degree two, which is forbidden in orientable non-Hermitian systems [19].

Gapless phases also have a characteristic signature in terms of oriented Fermi arcs. In phases with non-zero total Abelianization, a non-zero number of Fermi arcs must cross a nonorientable boundary. Since Fermi arcs reverse their direction on such crossing, this adds  $\pm 2$  to the total number of outflowing arcs. This reflects the evenness requirement for the total Abelianized charge parity in Eq. (3).

In gapless phases, Fermi arcs can terminate at EPs. Using the orientation defined in the previous section, open Fermi arcs are oriented away from the most generic twofold EPs with square root dispersion, and towards their inverses, resembling flux lines or Dirac strings. Whereas a normal EP is the source of one real and one imaginary flux line, the monopole in the example given in Eq. (8) at  $\ell = 1$  is the source of two of each,



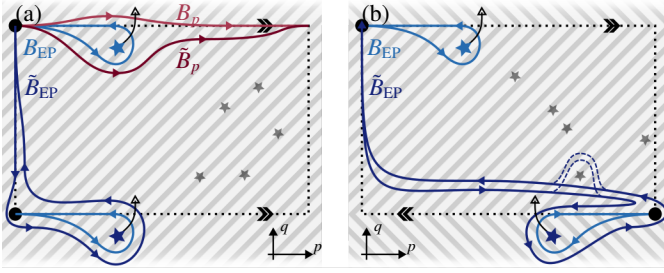


**Figure 3.** Rules for braided phase transitions. An EP (star marker) with braid invariant  $B_{EP}$ , measured along the light blue loop, crosses an (a) periodic ((b) anti-periodic) boundary. This leads to a phase transition from braid  $B_p$  (light red) to  $\tilde{B}_p = B_{EP}B_p$  (dark red) in both cases. The EP's braid invariant changes as well, transitioning according to Eq. (10). This can be understood by observing that an EP from the (anti-)periodic continuation moves into the fundamental domain as the original EP exits. This new EP carries the same (inverse) invariant, measured from the base point in the neighboring domain base point. The change in invariant to  $\tilde{B}_{EP}$  corresponds to a change of base point associated with the encircling trajectory. Potential other degeneracies (shaded black) can change this rule by additional conjugations if the EP encircles them before exiting the fundamental domain (dashed blue line in (b)); this follows the established non-Abelian braiding rules.

all oriented away from the EP, corresponding to its Abelianized braid charge 2. Both a nonzero number of total outflowing Fermi arcs, and a nonzero total Abelianization charge thus necessarily require a nonorientable fundamental domain.

*Braid Inversions and Phase Transitions.* — Under deformation of  $H(p, q)$ , EPs continuously move through the parameter space. This leads to phase transitions and charge inversions of the EP if it goes along the orientation-reversing direction in the parameter space.

We begin by deriving the rule for the phase transition. As shown in Figure 3, the braids along a loop in the parameter space before and after the EP crosses it differ precisely by the EP's braid  $B_{EP}$ . This implies the first rule of non-Hermitian phase transitions

$$B_{p,q} \rightarrow \tilde{B}_{p,q} = B_{EP}B_{p,q}, \quad (9)$$

which takes the same form for the orientable and nonorientable cases. Note that braids, as non-Abelian invariants, are base-point dependent. If the two braids are not measured on loops with the same base point as shown in Figure 3, the rule in Eq. (9) must be amended by a braid that accounts for this difference.

We continue by deriving how the charge of an EP changes  $B_{EP} \rightarrow \tilde{B}_{EP}$  when it encircles the parameter space along a loop. To make the picture clearer, we can think of the EP as exiting the fundamental domain into the neighboring unit cell on one side, while a partner EP enters the fundamental domain from the opposite side. These neighboring unit cells are [mirrored] copies of the fundamental domain if the crossed boundary is [non]orientable (see Figure 3). Thus, the partner EP that

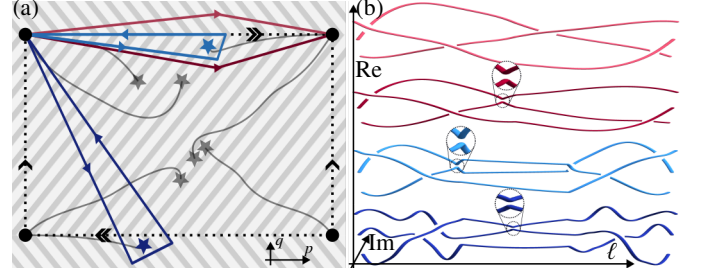


**Figure 4.** The braided phase transition on the Klein bottle described in Eq. (13). Increasing parameter  $t$  through critical  $t_0 \approx 0.29$ , the system transitions from phase  $(B_p^{\mathbf{K}^2}, B_q^{\mathbf{K}^2}) = (\sigma_2\sigma_1^{-1}, \Delta^{-1})$  to  $(\sigma_1^{-1}, \Delta^{-1})$ . (a) The parameter space for  $t = \frac{1}{4}$ , before the phase transition. Colored lines denote loops that determine the braids relevant to the transition, in line with Figure 3. Real Fermi arcs (black lines) terminate in EPs (stars). The light blue EP crosses the boundary, turning into the dark blue EP after the transition. (b) Spectral braiding along the loops shown in (a) in matching colors, parameterized along parameter  $\ell$ . Avoided crossings are highlighted. The light blue EP carries braid  $B_{EP} = \sigma_1^{-1}\sigma_2^{-1}\sigma_1^{-1}\sigma_2\sigma_1 = \sigma_2^{-1}$ . It moves across the  $p$ -boundary, changing the boundary braid from  $B_p = \sigma_1^{-1}\sigma_2^{-1}\sigma_1\sigma_2 = \sigma_2\sigma_1^{-1}$  determined along the light red path to  $\tilde{B}_p = \sigma_1^{-1}\sigma_2^{-1}\sigma_2 = \sigma_1^{-1}$  measured along the dark red path. In the transition, the EP charge changes to  $\tilde{B}_{EP} = \sigma_2\sigma_1\sigma_2^{-1}$  given in dark blue.

enters the fundamental domain carries the same [inverse] braid charge. However, this braid is measured from the base point of the neighboring unit cell. In order to describe the EP properly after it has entered the fundamental domain, we must re-base this invariant following

$$\tilde{B}_{EP} = B_{\text{rebase}} B_{EP}^{\pm 1} B_{\text{rebase}}^{-1}, \quad (10)$$

where the exponent is +1 if an orientable boundary is crossed, and -1 otherwise.

This change of base point from one unit cell to the next amounts to a conjugation by a braid  $B_{\text{rebase}}$ , which is given by the EP's trajectory around the parameter space (see Figure 3). If the EP encircles the spaces discussed here entirely, and its trajectory follows a loop that makes up a boundary, then this rebaseing can be given explicitly in terms of boundary braids as

$$B_{\text{rebase}} = \begin{cases} B_{pq}^{\mathbf{RP}^2} & \text{enc. } \mathbf{RP}^2, \\ B_p^{\mathbf{K}^2} & \text{enc. } \mathbf{K}^2, \text{ orientable direction,} \\ B_q^{\mathbf{K}^2} B_p^{\mathbf{K}^2} & \text{enc. } \mathbf{K}^2, \text{ nonorientable direction.} \end{cases} \quad (11)$$

If instead it follows a trajectory around other EPs in the space,  $B_{\text{rebase}}$  is amended by additional conjugating braids according to the usual rules of EP encircling.

We illustrate such a phase transition along a nonorientable direction in a Klein bottle model by tuning from  $H_{\text{gap}}^{\mathbf{K}^2}$  defined

in Eq. (6) to

$$H_{\text{gapless}}^{\mathbf{K}^2} = \begin{pmatrix} -a & 1 & 0 \\ 1 & b & 1 \\ 0 & 1 & a \end{pmatrix}, \text{ where } \begin{cases} a = i + ie^{2iq} \\ b = i(1 + \cos p) + \sin p \cos q \end{cases} \quad (12)$$

linearly, i.e.,

$$H_{\text{transition}}^{\mathbf{K}^2}(t) = (1-t)H_{\text{gap}}^{\mathbf{K}^2} + tH_{\text{gapless}}^{\mathbf{K}^2}, \quad (13)$$

As we show in Figure 4, this transition happens precisely according to the rules in Eqs. (9) and (10). Tuning away from the band-gapped model  $H_{\text{gap}}^{\mathbf{K}^2}$ , the gap closes and EPs are pair-created locally. One of these carries  $B_{\text{EP}} = \sigma_2^{-1}$  and crosses the boundary carrying  $B_p = \sigma_2\sigma_1^{-1}$ , which leads to a phase transition to  $\tilde{B}_p = \sigma_1^{-1}$ . After this phase transition, the EP carries a new invariant  $\tilde{B}_{\text{EP}} = \sigma_2\sigma_1\sigma_2^{-1}$ .

As the resulting topological phase carries  $\tilde{B}_{\text{tot}} = \sigma_2\sigma_1$ , this transition is from a gapped into a gapless phase. Note also that the resulting topological phase carries total Abelianization 2, which must originate in the nonorientable boundary. This means that any phase transition into a gapped phase must happen via crossing this nonorientable boundary, as it does in Eq. (13).

*Discussion.* — We have classified exceptional topological phases on two-dimensional nonorientable manifolds. We showed that gapped phases on the Klein bottle and real projective plane are determined by torsion and conjugacy problems in the braid group. These phases can be distinguished experimentally by their Fermi arcs, as in our explicit examples. We have

illustrated how telltale Fermi arc signatures arise and highlight EPs in gapless phases. These are closely associated to transitions of the braid when EPs encircle the parameter space in an orientation-preserving or orientation-reversing direction. Our work explores the interplay of exceptional and nonorientable phenomena, and paves the way to experimental observation of phenomena unique to such combined systems. Additional internal symmetries extend and amend the topological classification of non-Hermitian systems [14, 32, 63, 64], and even allow for the generic occurrence of higher-order EPs [65–67]; an investigation into their interplay with nonorientability would thus be of great future interest.

*Acknowledgments.* — JLKK acknowledges insightful discussions with Oscar Arandes, Lukas Rødland, and Tsuneya Yoshida. AGF, SV and MS acknowledge support from the U.S. Office of Naval Research (ONR) Multidisciplinary University Research Initiative (MURI) under Grant No. N00014-20-1-2325 on Robust Photonic Materials with Higher-Order Topological Protection. This material is based upon work also supported in part by the U.S. Army Research Office through the Institute for Soldier Nanotechnologies at MIT, under Collaborative Agreement Number W911NF-23-2-0121, and also in part by the Air Force Office of Scientific Research under the award number FA9550-21-1-0299. KY is supported by the ANR-DFG project (TWISTGRAPH). JLKK and EJB were supported by the Swedish Research Council (VR, grant 2018-00313), the Wallenberg Academy Fellows (2018.0460) and Scholars (2023.0256) programs, and the project Dynamic Quantum Matter (2019.0068) of the Knut and Alice Wallenberg Foundation, as well as the Göran Gustafsson Foundation for Research in Natural Sciences and Medicine.

- 
- [1] M. Berry, Physics of Nonhermitian Degeneracies, *Czechoslovak Journal of Physics* **54**, 1039 (2004).
  - [2] N. Moiseyev, *Non-Hermitian Quantum Mechanics* (Cambridge University Press, Cambridge ; New York, 2011).
  - [3] X. Zhu, H. Ramezani, C. Shi, J. Zhu, and X. Zhang,  $\mathcal{PT}$ -symmetric acoustics, *Phys. Rev. X* **4**, 031042 (2014).
  - [4] H. Zhou, C. Peng, Y. Yoon, C. W. Hsu, K. A. Nelson, L. Fu, J. D. Joannopoulos, M. Soljačić, and B. Zhen, Observation of bulk fermi arc and polarization half charge from paired exceptional points, *Science* **359**, 1009 (2018).
  - [5] A. Cerjan, S. Huang, M. Wang, K. P. Chen, Y. Chong, and M. C. Rechtsman, Experimental realization of a weyl exceptional ring, *Nature Photonics* **13**, 623 (2019).
  - [6] Y. Ashida, Z. Gong, and M. Ueda, Non-Hermitian physics, *Advances in Physics* **69**, 249 (2020).
  - [7] T. Helbig, T. Hofmann, S. Imhof, M. Abdelghany, T. Kiessling, L. Molenkamp, C. Lee, A. Szameit, M. Greiter, and R. Thomale, Generalized bulk–boundary correspondence in non-hermitian topoelectrical circuits, *Nature Physics* **16**, 747 (2020).
  - [8] T. Katō, *Perturbation Theory for Linear Operators*, Classics in Mathematics (Springer, Berlin, 1995).
  - [9] K. Ding, C. Fang, and G. Ma, Non-Hermitian topology and exceptional-point geometries, *Nat Rev Phys* **4**, 745 (2022).
  - [10] M.-A. Miri and A. Alù, Exceptional points in optics and photonics, *Science* **363**, eaar7709 (2019).
  - [11] A. Li, H. Wei, M. Cotrufo, W. Chen, S. Mann, X. Ni, B. Xu, J. Chen, J. Wang, S. Fan, *et al.*, Exceptional points and non-hermitian photonics at the nanoscale, *Nature Nanotechnology* **18**, 706 (2023).
  - [12] B. Zhen, C. W. Hsu, Y. Igarashi, L. Lu, I. Kaminer, A. Pick, S.-L. Chua, J. D. Joannopoulos, and M. Soljačić, Spawning rings of exceptional points out of dirac cones, *Nature* **525**, 354 (2015).
  - [13] H. Hodaei, A. U. Hassan, S. Wittek, H. Garcia-Gracia, R. El-Ganainy, D. N. Christodoulides, and M. Khajavikhan, Enhanced sensitivity at higher-order exceptional points, *Nature* **548**, 187 (2017).
  - [14] T. Yoshida, J. L. K. König, L. Rødland, E. J. Bergholtz, and M. Stålhammar, Winding topology of multifold exceptional points, *Phys. Rev. Res.* **7**, L012021 (2025).
  - [15] K. Ding, G. Ma, M. Xiao, Z. Q. Zhang, and C. T. Chan, Emergence, Coalescence, and Topological Properties of Multiple Exceptional Points and Their Experimental Realization, *Phys. Rev. X* **6**, 021007 (2016).
  - [16] H. B. Nielsen and M. Ninomiya, Absence of neutrinos on a lattice: (I). Proof by homotopy theory, *Nuclear Physics B* **185**, 20 (1981).

- [17] H. B. Nielsen and M. Ninomiya, Absence of neutrinos on a lattice: (II). Intuitive topological proof, *Nuclear Physics B* **193**, 173 (1981).
- [18] Z. Yang, A. P. Schnyder, J. Hu, and C.-K. Chiu, Fermion Doubling Theorems in Two-Dimensional Non-Hermitian Systems for Fermi Points and Exceptional Points, *Phys. Rev. Lett.* **126**, 086401 (2021).
- [19] J. L. K. König, K. Yang, J. C. Budich, and E. J. Bergholtz, Braid-protected topological band structures with unpaired exceptional points, *Phys. Rev. Res.* **5**, L042010 (2023).
- [20] T. E. Lee, Anomalous Edge State in a Non-Hermitian Lattice, *Phys. Rev. Lett.* **116**, 133903 (2016).
- [21] S. Yao and Z. Wang, Edge states and topological invariants of non-Hermitian systems, *Phys. Rev. Lett.* **121**, 086803 (2018).
- [22] F. K. Kunst, E. Edvardsson, J. C. Budich, and E. J. Bergholtz, Biorthogonal Bulk-Boundary Correspondence in Non-Hermitian Systems, *Phys. Rev. Lett.* **121**, 026808 (2018).
- [23] E. J. Bergholtz, J. C. Budich, and F. K. Kunst, Exceptional topology of non-Hermitian systems, *Rev. Mod. Phys.* **93**, 015005 (2021).
- [24] N. Okuma and M. Sato, Non-Hermitian Topological Phenomena: A Review, *Annual Review of Condensed Matter Physics* **14**, 83 (2023).
- [25] J. Ren and N. A. Sinitsyn, Braid group and topological phase transitions in nonequilibrium stochastic dynamics, *Phys. Rev. E* **87**, 050101 (2013).
- [26] H. Shen, B. Zhen, and L. Fu, Topological Band Theory for Non-Hermitian Hamiltonians, *Phys. Rev. Lett.* **120**, 146402 (2018).
- [27] C. C. Wojcik, X.-Q. Sun, T. Bzduszek, and S. Fan, Homotopy characterization of non-hermitian hamiltonians, *Phys. Rev. B* **101**, 205417 (2020).
- [28] Z. Li and R. S. K. Mong, Homotopical characterization of non-Hermitian band structures, *Phys. Rev. B* **103**, 155129 (2021).
- [29] H. Hu and E. Zhao, Knots and Non-Hermitian Bloch Bands, *Phys. Rev. Lett.* **126**, 010401 (2021).
- [30] K. Wang, A. Dutt, C. C. Wojcik, and S. Fan, Topological complex-energy braiding of non-Hermitian bands, *Nature* **598**, 59 (2021).
- [31] Q. Zhang, Y. Li, H. Sun, X. Liu, L. Zhao, X. Feng, X. Fan, and C. Qiu, Observation of acoustic non-Hermitian Bloch braids and associated topological phase transitions, *Phys. Rev. Lett.* **130**, 017201 (2023).
- [32] K. Yang, Z. Li, J. L. K. König, L. Rødland, M. Stålhammar, and E. J. Bergholtz, Homotopy, symmetry, and non-Hermitian band topology, *Rep. Prog. Phys.* **87**, 078002 (2024), arXiv:2309.14416 [cond-mat].
- [33] E. J. Pap, D. Boer, and H. Waalkens, Non-abelian nature of systems with multiple exceptional points, *Phys. Rev. A* **98**, 023818 (2018).
- [34] Y. S. S. Patil, J. Höller, P. A. Henry, C. Guria, Y. Zhang, L. Jiang, N. Kralj, N. Read, and J. G. E. Harris, Measuring the knot of non-Hermitian degeneracies and non-commuting braids, *Nature* **607**, 271 (2022).
- [35] C.-X. Guo, S. Chen, K. Ding, and H. Hu, Exceptional Non-Abelian Topology in Multiband Non-Hermitian Systems, *Phys. Rev. Lett.* **130**, 157201 (2023).
- [36] J. Zhong, C. C. Wojcik, D. Cheng, and S. Fan, Numerical and theoretical study of eigenenergy braids in two-dimensional photonic crystals, *Phys. Rev. B* **108**, 195413 (2023).
- [37] Y. Fu and Y. Zhang, Braiding topology of non-hermitian open-boundary bands, *Phys. Rev. B* **110**, L121401 (2024).
- [38] C. Guria, Q. Zhong, S. K. Ozdemir, Y. S. Patil, R. El-Ganainy, and J. G. E. Harris, Resolving the topology of encircling multiple exceptional points, *Nat. Commun.* **15**, 1369 (2024).
- [39] Y. Long, Z. Wang, C. Zhang, H. Xue, Y. X. Zhao, and B. Zhang, Non-abelian braiding of topological edge bands, *Phys. Rev. Lett.* **132**, 236401 (2024).
- [40] K. Wang, J. L. K. König, K. Yang, L. Xiao, W. Yi, E. J. Bergholtz, and P. Xue, *Photonic Non-Abelian Braid Monopole* (2024), arXiv:2410.08191 [cond-mat].
- [41] A. Grossi e Fonseca, S. Vaidya, T. Christensen, M. C. Rechtsman, T. L. Hughes, and M. Soljačić, Weyl Points on Nonorientable Manifolds, *Phys. Rev. Lett.* **132**, 266601 (2024).
- [42] Z. Y. Chen, S. A. Yang, and Y. X. Zhao, Brillouin Klein bottle from artificial gauge fields, *Nat Commun* **13**, 2215 (2022).
- [43] C.-A. Li, J. Sun, S.-B. Zhang, H. Guo, and B. Trauzettel, Klein-bottle quadrupole insulators and Dirac semimetals, *Phys. Rev. B* **108**, 235412 (2023).
- [44] Z. Pu, H. He, W. Deng, X. Huang, L. Ye, J. Lu, M. Ke, and Z. Liu, Acoustic Klein bottle insulator, *Phys. Rev. B* **108**, L220101 (2023).
- [45] Y.-L. Tao, M. Yan, M. Peng, Q. Wei, Z. Cui, S. A. Yang, G. Chen, and Y. Xu, Higher-order Klein bottle topological insulator in three-dimensional acoustic crystals, *Phys. Rev. B* **109**, 134107 (2024).
- [46] Z. Zhu, L. Yang, J. Wu, Y. Meng, X. Xi, B. Yan, J. Chen, J. Lu, X. Huang, W. Deng, C. Shang, P. P. Shum, Y. Yang, H. Chen, K. Xiang, G.-G. Liu, Z. Liu, and Z. Gao, Brillouin Klein space and half-turn space in three-dimensional acoustic crystals, *Science Bulletin* **69**, 2050 (2024).
- [47] Y. Wang, C. Zhang, Z. Y. Chen, B. Liang, Y. X. Zhao, and J. Cheng, *Chess-board Acoustic Crystals with Momentum-space Nonsymmorphic Symmetries* (2023), arXiv:2305.07174 [cond-mat].
- [48] J. Hu, S. Zhuang, and Y. Yang, Higher-Order Topological Insulators via Momentum-Space Nonsymmorphic Symmetries, *Phys. Rev. Lett.* **132**, 213801 (2024).
- [49] C. Shang, S. Liu, C. Jiang, R. Shao, X. Zang, C. H. Lee, R. Thomale, A. Manchon, T. J. Cui, and U. Schwingenschlögl, Observation of a Higher-Order End Topological Insulator in a Real Projective Lattice, *Advanced Science* **11**, 2303222 (2024).
- [50] P. Lai, J. Wu, Z. Pu, Q. Zhou, J. Lu, H. Liu, W. Deng, H. Cheng, S. Chen, and Z. Liu, Real-projective-plane hybrid-order topological insulator realized in phononic crystals, *Phys. Rev. Appl.* **21**, 044002 (2024).
- [51] C. Zhang, Z. Y. Chen, Z. Zhang, and Y. X. Zhao, General Theory of Momentum-Space Nonsymmorphic Symmetry, *Phys. Rev. Lett.* **130**, 256601 (2023).
- [52] T. Morimoto, H. C. Po, and A. Vishwanath, Floquet topological phases protected by time glide symmetry, *Phys. Rev. B* **95**, 195155 (2017).
- [53] X. Shen, K. Pan, X. Wang, and X. Zhou, *Observation of Klein bottle quadrupole topological insulators in electric circuits* (2024), arXiv:2407.07470 [cond-mat].
- [54] D. Călugăru, Y. Jiang, H. Hu, H. Pi, J. Yu, M. G. Vergniory, J. Shan, C. Felser, L. M. Schoop, D. K. Efetov, K. F. Mak, and B. A. Bernevig, *A New Moiré Platform Based on M-Point Twisting* (2024), arXiv:2411.18684 [cond-mat].
- [55] E. Artin, Theorie der Zöpfe, *Abh.Math.Semin.Univ.Hambg.* **4**, 47 (1925).
- [56] K. Wang, A. Dutt, C. C. Wojcik, and S. Fan, Topological complex-energy braiding of non-hermitian bands, *Nature* **598**,

- 59 (2021).
- [57] F. E. Öztürk, T. Lappe, G. Hellmann, J. Schmitt, J. Klaers, F. Vewinger, J. Kroha, and M. Weitz, Observation of a non-hermitian phase transition in an optical quantum gas, *Science* **372**, 88 (2021).
- [58] A. Bergman, R. Duggan, K. Sharma, M. Tur, A. Zadok, and A. Alù, Observation of anti-parity-time-symmetry, phase transitions and exceptional points in an optical fibre, *Nature communications* **12**, 486 (2021).
- [59] M.-A. Miri and A. Alu, Exceptional points in optics and photonics, *Science* **363**, eaar7709 (2019).
- [60] C. Kassel and V. Turaev, *Braid Groups*, Graduate Texts in Mathematics, Vol. 247 (Springer New York, New York, NY, 2008).
- [61] W. Tang, X. Jiang, K. Ding, Y.-X. Xiao, Z.-Q. Zhang, C. T. Chan, and G. Ma, Exceptional nexus with a hybrid topological invariant, *Science* **370**, 1077 (2020).
- [62] H. Zhou, C. Peng, Y. Yoon, C. W. Hsu, K. A. Nelson, L. Fu, J. D. Joannopoulos, M. Soljačić, and B. Zhen, Observation of bulk Fermi arc and polarization half charge from paired exceptional points, *Science* **359**, 1009 (2018).
- [63] D. Bernard and A. LeClair, A classification of non-hermitian random matrices, in *Statistical Field Theories*, edited by A. Capelli and G. Mussardo (Springer Netherlands, Dordrecht, 2002) pp. 207–214.
- [64] K. Kawabata, K. Shiozaki, M. Ueda, and M. Sato, Symmetry and Topology in Non-Hermitian Physics, *Phys. Rev. X* **9**, 041015 (2019).
- [65] P. Delplace, T. Yoshida, and Y. Hatsugai, Symmetry-Protected Multifold Exceptional Points and Their Topological Characterization, *Phys. Rev. Lett.* **127**, 186602 (2021).
- [66] I. Mandal and E. J. Bergholtz, Symmetry and Higher-Order Exceptional Points, *Phys. Rev. Lett.* **127**, 186601 (2021).
- [67] S. Sayyad and F. K. Kunst, Realizing exceptional points of any order in the presence of symmetry, *Phys. Rev. Research* **4**, 023130 (2022).